

Probing the Origin of Viscosity of Liquid Electrolytes for Lithium Batteries

Nao Yao, Legeng Yu, Zhong-Heng Fu, Xin Shen, Ting-Zheng Hou, Xinyan Liu, Yu-Chen Gao, Rui Zhang, Chen-Zi Zhao, Xiang Chen,* and Qiang Zhang*

Abstract: Viscosity is an extremely important property for ion transport and wettability of electrolytes. Easy access to viscosity values and a deep understanding of this property remain challenging yet critical to evaluating the electrolyte performance and tailoring electrolyte recipes with targeted properties. We proposed a screened overlapping method to efficiently compute the viscosity of lithium battery electrolytes by molecular dynamics simulations. The origin of electrolyte viscosity was further comprehensively probed. The viscosity of solvents exhibits a positive correlation with the binding energy between molecules, indicating viscosity is directly correlated to intermolecular interactions. Salts in electrolytes enlarge the viscosity significantly with increasing concentrations while diluents serve as the viscosity reducer, which is attributed to the varied binding strength from cation–anion and cation–solvent associations. This work develops an accurate and efficient method for computing the electrolyte viscosity and affords deep insight into viscosity at the molecular level, which exhibits the huge potential to accelerate advanced electrolyte design for next-generation rechargeable batteries.

Introduction

Dynamic viscosity (η), usually referred to as viscosity, is a fundamental and extremely important physical property of liquids. It describes the resistance of a liquid to flow and plays a significant role in various applications involving liquids such as lubricating oils, printing inks, and biological agents. Liquid electrolyte is a representative liquid system and is particularly focused on herein as it is a critical component of rechargeable lithium batteries that have achieved wide applications in our daily life and are promising in constructing future sustainable energy systems.^[1]

As a crucial property of the liquid electrolyte, viscosity highly affects the electrolyte and battery performance. On the one hand, viscosity is closely related to electrolyte transport properties, such as ionic diffusivity, conductivity, and transference number. According to the Stokes–Einstein equation and the Nernst–Einstein equation, viscosity varies inversely with diffusion coefficient and ionic conductivity.^[2] Consequently, high ionic conductivity, which is a principal requirement for electrolytes with low ion transport resistance and batteries with high-rate capability, calls for low viscosity.^[3,4] The application of batteries in harsh scenarios such as low-temperature or fast-charging conditions especially appeals to electrolytes for satisfying such requirements.^[4,5] Besides, previous studies found that the solvent viscosity overweighed the ion aggregation and cation transference number in influencing the ionic transport, highlighting the significance of the electrolyte viscosity.^[6] On the other hand, viscosity affects the electrolyte wettability to the separator and electrode in a battery.^[7,8] The wetting of a drop on the solid surface is generally slower for highly viscous liquids than that for low-viscosity liquids.^[9] A low-viscosity electrolyte is generally desired to achieve excellent wettability for stable injection and pre-formation processes during the assembling of batteries, especially high-energy-density ones which demand lean electrolytes. As a result, electrolyte viscosity is an indispensable property to be considered when designing advanced electrolytes for practical applications.

Tremendous efforts have been devoted to probing electrolyte viscosity,^[10,11] which generally involve obtaining the viscosity of a specific electrolyte or solvent to evaluate its potential applicability in batteries and understanding the structure–function relationship between the electrolyte structure and viscosity to achieve a rational design of electrolyte components. Specifically, the experimental meas-

[*] N. Yao, L. Yu, Dr. Z.-H. Fu, Dr. X. Shen, Y.-C. Gao, Dr. C.-Z. Zhao, Dr. X. Chen, Prof. Q. Zhang

Beijing Key Laboratory of Green Chemical Reaction Engineering and Technology, Department of Chemical Engineering, Tsinghua University

Beijing 100084 (China)

E-mail: xiangchen@mail.tsinghua.edu.cn

zhang-qiang@mails.tsinghua.edu.cn

Dr. T.-Z. Hou

Department of Materials Science and Engineering, University of California

Berkeley, CA 94720 (USA)

Dr. X. Liu

Institute of Fundamental and Frontier Sciences, University of Electronic Science and Technology of China

Chengdu 611731, Sichuan (China)

Dr. R. Zhang

School of Materials Science and Engineering, Advanced Research Institute for Multidisciplinary Science, Beijing Institute of Technology

Beijing 100081 (China)

urement of viscosity is facile but neither economical nor efficient. In addition, conventional experiments start with an established electrolyte recipe and then test its viscosity, followed by adjusting the recipe to suit specific requirements. Such trial-and-error methods have difficulty in gaining a deep insight into viscosity and tailoring electrolyte molecules rationally. Computational techniques afford an alternative to obtain viscosity efficiently and even in a high-throughput way.^[12]

Among various methods for computing the viscosity of liquids, coupling equilibrium molecular dynamics (EMD) simulations with the Green–Kubo (GK) formula^[13] or the reformulated Einstein relation^[14] is widely used due to its simplicity, but this method demands adequate sampling and delicate data-processing to achieve good results.^[15] Different strategies have been accordingly proposed to determine the viscosity accurately, including adopting the average value of a certain period of the integral as viscosity,^[16] taking the integral of pressure tensor autocorrelation function over a cutoff time,^[17] conducting multiple independent simulations to compute viscosities and averaging over them,^[18,19] and fitting the simulation data with a certain function to calculate viscosity.^[20] However, these approaches depend more or less on arbitrary parameters such as the cutoff time and the form of the fitting function, and different viscosities can be obtained for the same system depending on these parameters. Zhang et al. recently proposed a time decomposition approach to objectively yield viscosity, which though requires complicated steps and iterations.^[21] In addition, previous computational research on viscosity lacks in-depth digging into the simulation data. Models comprised of atoms and molecules are used to simulate macroscopic electrolyte systems in MD simulations. Based on detailed analyses, a molecular-level understanding of viscosity is supposed to be within easy access, which benefits designing molecules from the bottom to formulate electrolytes with suitable viscosity.

In this contribution, an accurate and efficient screened overlapping method (SOM) was developed to compute the viscosity of liquid electrolytes by MD simulations. SOM takes only three easily-implemented steps. It determines an appropriate correlation time and couples the screening of fluctuated results for the first time, giving rise to superior accuracy and time performance compared with literature methods. The influences of electrolyte components and their ratios on viscosity were further systematically analyzed and discussed. A positive relationship between the binding energy of molecules and the electrolyte viscosity was discovered. The addition of salts increases the electrolyte viscosity rapidly due to the much stronger interaction between cations and anions in salts than that between solvent molecules, as well as the formation of solvation structures that prevent solvents from free motion. Diluents can moderate the high viscosity of concentrated electrolytes due to their relatively low viscosity and their role in breaking ion clusters to lessen the overall association between electrolyte components. This work not only provides a computational approach for obtaining the electrolyte viscosity efficiently but also reveals the intrinsic

connection between viscosity and intermolecular interactions. The molecular understanding of viscosity affords a basis for the modification or creation of molecular structures and electrolytes, paving a novel paradigm for designing functional electrolytes.

Results and Discussion

Model and Method Development for Computing Viscosity

Viscosity can be obtained from stress fluctuations in an EMD simulation according to the GK formula. The GK formula can be further formulated as an Einstein relation:^[15]

$$\eta = \lim_{t \rightarrow \infty} \frac{1}{2} \frac{V}{k_B T} \frac{d}{dt} \left\langle \left(\int_{t_0}^{t_0+\Delta t} P_{xy}(t) dt \right)^2 \right\rangle_{t_0} \quad (1)$$

where η , V , k_B , T , P , Δt , and t are the viscosity, volume of the system, Boltzmann constant, temperature, shear stress tensor, integral time, and total simulation time, respectively. The Einstein relation considers integrals over short times, and the inaccuracies of the long-time correlations in the original GK formula can be ignored.^[22] Therefore, it is more convenient to compute viscosity based on the Einstein relation than the original GK formula in practice. Additionally, the GK formula is based on the linear response theory (LRT). LRT gives the nonequilibrium response of a system to an external perturbation by equilibrium correlation functions supposing that the perturbation is very weak, which corresponds to very low shear rates applied to obtain the zero-shear-rate viscosity, namely the constant viscosity in the limit of zero shear rate, in experimental measurements. Therefore, the calculated viscosity by the Einstein relation (or the GK formula) can be considered the zero-shear-rate viscosity, which applies to both Newtonian and non-Newtonian fluids. In batteries, electrolytes usually do not undergo shearing and stay at rest, which is consistent with the state of zero-shear-rate viscosity. Zero-shear-rate viscosity is thus applicable to electrolyte and battery applications.

We put forward a screened overlapping method (SOM) for the accurate and efficient computation of viscosity which is straightforward in practice without intricate procedures. Method details are stated as follows:

- (1) Determine the integral time (Δt): The Einstein relation considers integrals over short time intervals. Therefore, the change in calculated viscosities of two solvents, dimethyl carbonate (DMC, $\eta_{\text{exp.,298 K}} = 0.59 \text{ mPa s}$)^[23] and ethylene carbonate (EC, $\eta_{\text{exp.,313 K}} = 1.90 \text{ mPa s}$)^[23] whose experimental viscosities are distinct, with different time intervals was first probed to determine a reasonable integral interval. The viscosities of both DMC and EC rise with increasing time intervals at first, and then they converge at approximately 50 ps (Figure S1). This trend shares the same principle as the behavior of the shear stress tensor autocorrelation function in the GK equation which gradually decays to zero with increasing time, followed by a heavier fluctuation around zero

over a longer time.^[18] To avoid the increasing statistical error for longer correlation times, the timing at which viscosities start to converge, i.e., 50 ps, was selected as the integral time. The stress tensor can be integrated every 50 ps and averaged to produce the viscosity with the simulation time. Since the total simulation time is split into fragments of 50 ps each, this method is denoted as the splitting method (SM, Figure 1A). Besides DMC and EC, the viscosities of routine carbonates and ethers used for battery electrolytes, including ethyl acetate (EA), 1,2-dimethoxyethane (DME), 1,3-dioxolane (DOL), ethyl methyl carbonate

(EMC), diethyl carbonate (DEC), and fluoroethylene carbonate (FEC), were all calculated by SM (Figure 1B and Figure S2). The viscosities converge with increasing time, and values at the end of simulations were the SM viscosities (η_{SM}).

- (2) Ensure adequate sampling: η_{SM} evidently deviates from experimental values, especially for large-viscosity solvents. We speculated that this is due to the statistically demanding computation of viscosity. The total simulation run was then divided into N samples, each with a

duration of t/N ($t/N > 50$ ps), to simultaneously meet the 50 ps integral requirement and enhance sampling as much as possible. Within each sample, the integral evolves every 1 fs and the viscosity is the average of

$t/N\Delta t + 1$ integrals. As the simulation data in different intervals are overlapped, this method was named the overlapping method (OM, Figure 1A). The median of the N samples is statistically considered a reliable value,^[19] namely the OM viscosity (η_{OM}).

- (3) Screen divergent results and get the viscosity: Among the total N samples in OM, some of them fluctuated heavily and did not converge (Figure S3). As a result, η_{OM} are still not comparable to experimental viscosities in some cases (Figure 1B). A standard deviation threshold equal to 10 % of the mean value of the N samples was set with the purpose of screening divergent samples (Figure S3). The median value of the remaining samples is determined to be the final viscosity (Figure 1b and Figure S4). The above three steps give a completely integrated method for computing viscosity, screened overlapping method (SOM).

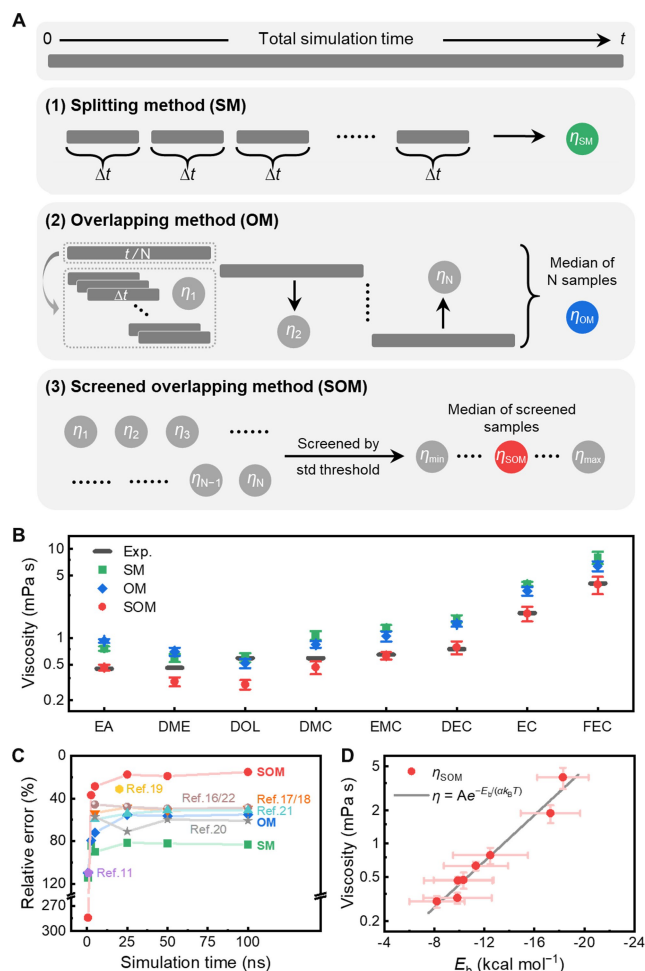


Figure 1. The computation methods for viscosity (η) and the summary of viscosities and binding energies (E_b) of pure solvents. A) Schematic of the computation methods for viscosity. t , Δt , and N are the total simulation time, the integral time, and the number of divided samples, respectively. Std stands for standard deviation. B) Comparison of calculated viscosities of pure solvents with experimental results.^[23,24] C) Relative error and time performance comparisons between SM, OM, SOM, and literature methods.^[11,16,17,18–22] The numbers indicate corresponding reference indexes. D) Correlation between the viscosity and the binding energy between solvent molecules. The error bars of η and relative error are defined as the standard deviation of viscosities of multiple parallel simulations for each system, while the error bar of E_b is the standard deviation calculated as stated in the Method part in Supporting Information.

Viscosity of Pure Solvents

The as-calculated viscosities of pure solvents show stepwise improvement in accuracy in the order of SM, OM, and SOM (Figure 1B and Figure S5). The solvent viscosities produced by SM and OM all show relative errors (δ) larger than 30 % with respect to experimental values except for that of DOL. The δ of DEC even reaches up to 118 % and 90 % for SM and OM, respectively. In comparison, the SOM viscosity (η_{SOM}) agrees the best with experiment values as the δ for all solvents except for DOL are the smallest among the three methods, especially those for EA, EMC, DEC, EC, and FEC, which are smaller than ± 5 %. The large relative error of DOL can be attributed to the inaccuracy of MD force field parameters. The intermolecular binding energies calculated by the MD simulation and high-accuracy density functional theory calculation show that MD underestimates the interaction strength between DOL molecules (Figure S6), giving rise to the much lower viscosity of DOL compared to experimental values.

Moreover, the accuracy and time performances of SOM were compared with literature methods (Figure 1C).^[11,16,17,18–22] SOM outperforms all other methods as long as the simulation time exceeds 2.5 ns, and its accuracy continues to improve with increasing time. In contrast,

literature methods sustain a low-accuracy level regardless of simulation time. With a total 100 ns simulation, SOM exhibits an average δ of about 15 %, which is more accurate by 15 % than the most precise results from Yamaguchi et al.^[19] among literature methods. Previous studies also demonstrated the superiority of nonequilibrium MD (NEMD) simulations over EMD in calculating the viscosities of Lennard–Jones fluids and water.^[15,22,25] However, the comparison between SOM and the NEMD-based periodic perturbation method (NEMD-PPM), which performed best among various EMD and NEMD methods according to Hess et al.,^[22] shows that the NEMD-PPM viscosities of solvents deviate larger from experimental values than those by SOM except for DOL (Figure S7). These all indicate the high reliability and efficiency of the proposed SOM.

Different solvents can present distinct viscosities. Taking EC and FEC as an example, they both belong to the carbonate solvents and share similar molecular structures, but their viscosities differ from each other. The binding energy (E_b) between solvent molecules was further calculated by analyzing the MD-based potential energy of molecules to rationalize this phenomenon. The viscosity of solvents is positively correlated with the binding energy, which can be well described by an exponential function (Figure 1D):

$$\eta = Ae^{\frac{E_b}{\alpha k_B T}} \quad (2)$$

where A and α are pre-exponential and exponent fitting coefficients, respectively, and T equals 298.15 K (Table S1). The definition of viscosity states that viscosity arises from the friction between liquid layers, and such friction forces originate from interactions between molecules. Consequently, a larger binding energy corresponds to a stronger interaction, inducing a larger friction force and a higher viscosity. The exponential relationship also suggests that minor increases in the binding energy between molecules will trigger noticeable changes in viscosity, implying the sensitivity of this property. It should also be noted that the binding energy between DOL molecules is the smallest among all solvents, which is in sync with the lowest computed viscosity of DOL.

Viscosity of Binary Solvent Mixtures

Solvent mixtures are more frequently used in electrolytes than pure solvents to take advantage of different species, represented by the mixture of linear and cyclic carbonates such as EC/DMC. The less viscous DMC counteracts the high viscosity of EC (Figure 2A). Nonetheless, the viscosities of EC/DMC mixtures with different ratios are not subject to a linear superposition of the respective viscosities of EC and DMC. EC/DMC mixtures exhibit a negative deviation from the simple addition rule. For instance, the calculated viscosity of EC/DMC with a 1:1 molar ratio is 0.91 mPas while the value obtained from linear addition is 1.25 mPas. Parameters a and b , which are fitted based on calculated viscosities of solvent mixtures at different mixing

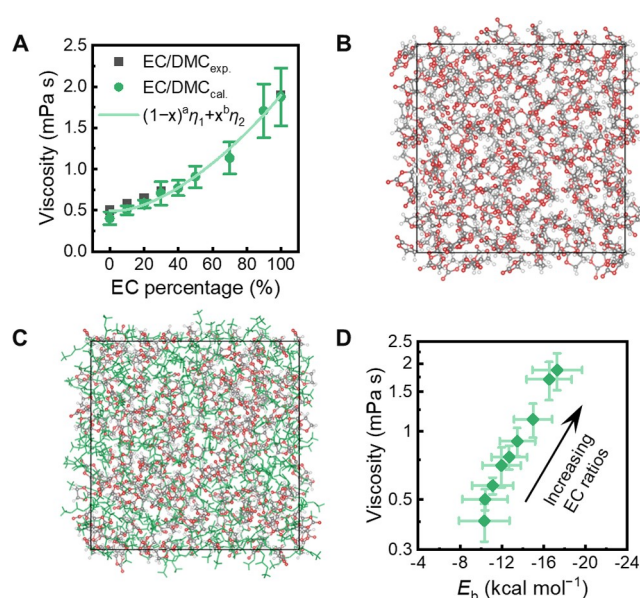


Figure 2. The viscosities and binding energies of EC/DMC binary solvent mixtures with different mixing ratios. A) The computed and experimental viscosities of EC/DMC mixtures with varied EC molar percentages. The MD snapshot of B) pure EC solvents and C) EC/DMC mixtures with a molar ratio of 1:1. EC molecules are represented by colored ball sticks while DMC molecules are represented by green sticks. Color mapping for elements: H-white, C-gray, O-red. D) The correlation between the viscosities and binding energies in EC/DMC mixtures.

ratios, were then introduced to the linear superposition model, forming the exponentially weighted linear superposition model to represent the viscosity of binary solvent mixtures (Table S2):

$$\eta = (1-x)^a \eta_1 + x^b \eta_2 \quad (3)$$

where $(1-x)$ and x are the molar fractions of two individual solvent components. Parameters a and b indicate the deviation of intermolecular interactions in solvent mixtures compared with those in pure solvents. The former is weaker than the latter, resulting in the negative deviation of practical viscosities relative to linear-mixing viscosities.

MD snapshots of pure EC and EC/DMC mixtures further visualize the effects brought by mixing these two solvents. The added DMC molecules uniformly distribute in EC molecules and break the strong interactions between EC (Figure 2B and C). This results in the overall weakened binding energy from -17.28 to -10.33 kcal mol $^{-1}$ and the reduced viscosity from 1.88 to 0.40 mPas as the EC ratio decreases (Figure 2D). Other binary mixtures including EC/EMC and FEC/DMC were also probed. Their viscosities follow a similar nonlinear rule as EC/DMC, and the increasing percentage of DMC or EMC in the mixture decreases the average binding energy between molecules and the viscosity (Figures S8 and S9).

Viscosity of Practical Electrolytes

Apart from solvent systems, the mixture of salts and solvents, namely electrolytes, is another significant category of liquids. The addition of salts into solvents has drastic effects on the liquid properties, and therefore viscosity of practical electrolytes is further considered to acquire a comprehensive insight into the viscosity. Especially, high-concentration electrolytes (HCEs) have surged in recent years for their excellent compatibility with high-capacity lithium metal anodes, while the large viscosity of HCEs is a major concern in terms of practical applications.^[26–28] Herein DMC/LiFSI electrolytes with different salt concentrations are taken as a representative example owing to the extensive research on this recipe (Figure 3A).^[28–31] The viscosities of DMC/LiFSI computed by SOM rise exponentially as the salt concentration increases, reproducing the rapid growth trend observed in experiments (Figure 3B).^[29] Specifically, the 1.1 M DMC/LiFSI electrolyte possesses a viscosity of 1.89 mPa s, and this value increases to 19.61 mPa s in the 3.1 M electrolyte counterpart. When the salt concentration reaches 4.9 M, the viscosity is about four times the viscosity at 3.1 M. On the one hand, salt is an infinitely viscous material. The stronger cation–anion binding strength than solvent–solvent binding strength naturally endows the electrolyte with an increased viscosity.^[32] On the other hand,

solvation structures are formed in electrolytes in the presence of salts. Specifically, the ratio of solvents in Li^+ solvation shells increases from 31 % to nearly 100 % as the salt concentration increases from 1.1 to 4.9 M (Figure S10). The continuously added cation–solvent interactions intensify the average binding strength in the electrolyte to induce a high viscosity. As a result of the formation of solvation structures, solvent molecules are constrained and their diffusion coefficients (D) encounter orders-of-magnitude decline which reflects the increased viscosity as well (Figure 3C).

Apart from solvation structures composed of solvents, contact ion pairs (CIPs), aggregates (AGGs), and large ion clusters are frequently observed in concentrated electrolytes (Figure 3D and Figure S11).^[27,28,33] The more concentrated the electrolyte is, the larger the cluster size becomes, and the larger proportion the bulky ion clusters account for (Figure 3E). In 1.1 and 1.7 M DMC/LiFSI electrolytes, the ion cluster size disperses over a wide range. The distribution concentrates around the maximum number of Li^+ in simulation systems when the salt concentration continues to increase, namely 50, 67, 100, and 133 in 2.5, 3.1, 4.1, and 4.9 M electrolytes, respectively. Both Li^+ and FSI^- diffuse slower accordingly (Figure S12). Generally, the cation–anion and cation–solvent interactions in addition to the solvent–solvent interactions make electrolyte components bind more

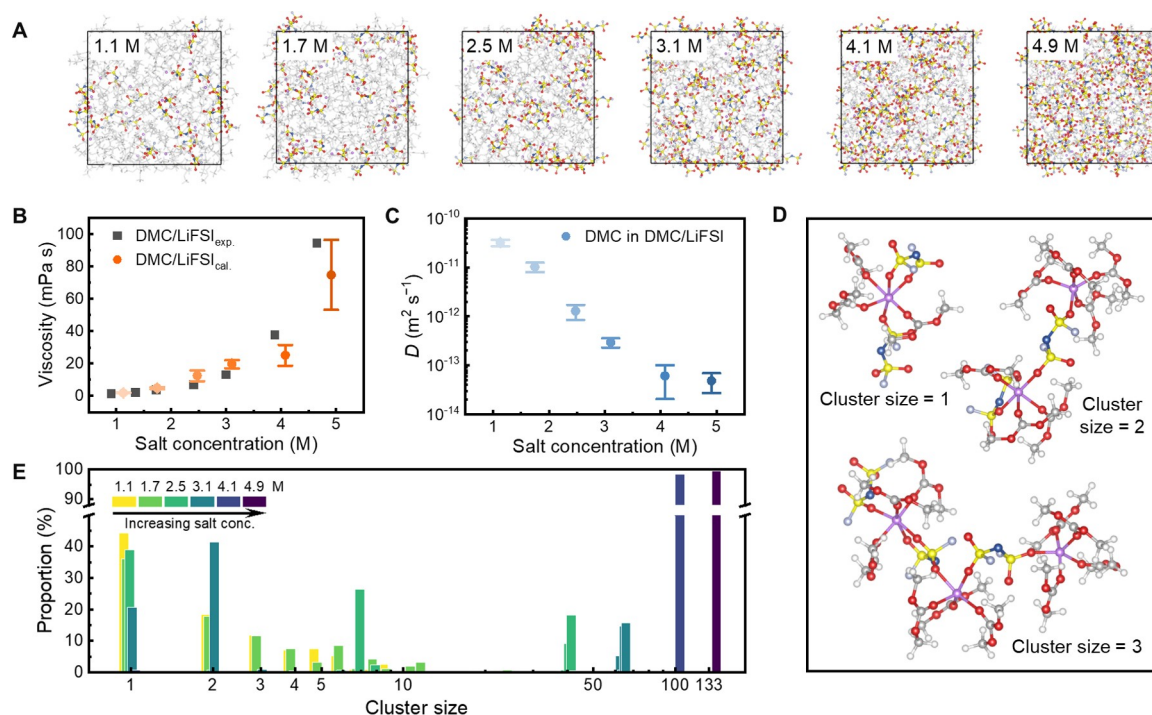


Figure 3. The MD snapshots, viscosities, diffusion coefficients, and solvation structure statistics of DMC/LiFSI electrolytes with different salt concentrations. A) MD snapshots of DMC/LiFSI electrolytes with salt concentration ranging from 1.1 to 4.9 M. Li^+ and FSI^- are shown in colored ball sticks while DMC solvents are shown in white sticks. Color mapping for elements: Li-violet, N-blue, O-red, F-light purple, S-yellow. B) Comparison of computed and experimental^[29] electrolyte viscosities. C) Diffusion coefficient (D) evolution of DMC solvents as the salt concentration increases. The error bars of D represent the standard deviation of D of multiple parallel simulations for each system. D) Extracted solvation structures with cluster sizes equaling 1, 2, and 3, where the cluster size is defined as the number of Li^+ in isolated Li^+ – FSI^- –DMC clusters. Color mapping for elements: H-white, Li-violet, C-gray, N-blue, O-red, F-light purple, S-yellow. E) Cluster size distribution in DMC/LiFSI electrolytes with increasing salt concentrations.

tightly than those in systems without salts. This effect is even intensified with increasing salt concentrations. The transport of both ions and solvents is retarded, and the viscosity displays a significant growth trend (Figure S13).

To address the high-viscosity weakness of HCEs, diluents that possess weak solvating power and low viscosity are introduced, forming localized high-concentration electrolytes (LHCEs, Figure 4A).^[34] 1,1,2,2-tetrafluoroethyl-2,2,3,3-tetrafluoropropylether (TTE), a representative diluent, was added into 4.9 M DMC/LiFSI to probe the critical role of diluents in regulating electrolyte solvation structures and viscosities. As expected, TTE helps to lower the electrolyte viscosity from nearly 80 mPa s to less than 10 mPa s as the ratio of TTE to DMC increases from 0 to 1.33, i.e., the salt concentration decreases from 4.9 to 2.0 M (Figure 4B).

It is well acknowledged that the addition of diluents into HCEs has little effect on electrolyte solvation structures ascribed to the non-solvating or low-solvating nature of

diluents.^[8,35] LHCEs are supposed to preserve the microscopic structures in HCEs. The percentage of coordinated DMC solvents indeed barely changes at different TTE ratios (Figure S14). However, the diffusion coefficient of DMC shows a pronounced increase by a factor of ten (Figure 4C). Detailed analyses on the solvation structure of DMC/LiFSI/TTE electrolytes prove the existence of large ion clusters as those in HCEs, but it is noted that a percentage of small-size ion complexes recur in 2.4 and 2.0 M TTE-containing LHCEs (Figure 4D). Therefore, diluents can break the cluster network at a high diluent ratio,^[29,30] which impairs the strong association between ions and solvents to some extent. Solvents in separated small complexes can move freely without burden as evidenced by more DMC molecules having a diffusion coefficient larger than $10^{-13} \text{ m}^2 \text{ s}^{-1}$ (Figure S15). Similarly, Li^+ and FSI^- , as well as TTE, also move faster in less concentrated electrolytes (Figure S16). Diluents function as molecular lubricants in the electrolyte. The weak interactions between diluent molecules, the absence of binding between diluents and ions, and the diminished association among ion clusters by diluents all contribute to the overall reduction of intermolecular frictions. Electrolyte components migrate easily, delivering a low viscosity (Figure S17).

Moreover, the correlation between the binding energy and viscosity of electrolytes and solvent mixtures can both be described by formula (2) (Table S1), which was summarized along with that of pure solvents in Figure S18. The fitting results of all these systems appear to resemble each other, abiding by a unifying principle. At the limit of zero binding energy, i.e., no intermolecular interactions, the system turns into an ideal gas, and the pre-exponential factor A in formula (2) corresponds to the viscosity of solvents in the ideal gas state, which is around 0.036 mPa s. The expression for the viscosity of an ideal gas was derived by Maxwell based on the rigid sphere model:^[36]

$$\mu = \frac{2}{3\pi} \frac{\sqrt{\pi m k_B T}}{\pi d^2} \quad (4)$$

where m and d are the mass and diameter of the sphere, respectively. The viscosities of pure solvents calculated based on this formula are around 0.005 to 0.006 mPa s (Table S3), which are comparable with the result (0.036 mPa s) obtained from the proposed formula (2) as these are all extremely low viscosities. Not only the feasibility of the exponential fitting but also the intrinsic relation between viscosity and molecular interactions is proved.

Additionally, the viscosity is highly dependent on the temperature, coming into play especially in all-climate applications. The temperature dependence of viscosities of one HCE system (4.9 M DMC/LiFSI) and one LHCE system (2.0 M DMC/LiFSI/TTE) was further probed (Figure S19). The electrolyte viscosities increase accordingly with the decreasing temperature, which can also be inferred from formula (2). Specifically, the viscosities of the HCE and LHCE systems increase from 47.40 to 112.74 mPa s and from 3.36 to 17.19 mPa s, respectively, when the temperature

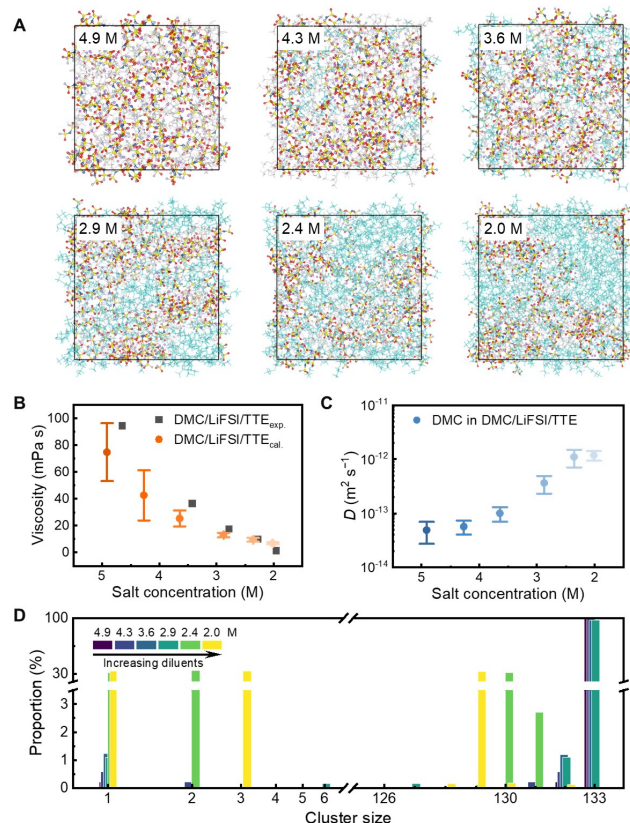


Figure 4. The MD snapshots, viscosities, diffusion coefficients, and solvation structure statistics of DMC/LiFSI/TTE electrolytes with different TTE diluent ratios, i.e., varied salt concentrations. A) MD snapshots of DMC/LiFSI/TTE electrolytes with the salt concentration ranging from 4.9 to 2.0 M. Li^+ and FSI^- are shown in colored ball sticks while DMC solvents and TTE diluents are shown in white and cyan sticks, respectively. Color mapping for elements: Li-violet, N-blue, O-red, F-light purple, S-yellow. B) Comparison of computed and experimental^[29] electrolyte viscosities. C) D evolution of DMC solvents as the salt concentration increases. D) Cluster size distribution in DMC/LiFSI/TTE electrolytes with increasing diluent ratios.

decreases from 328 to 243 K. This indicates that high-performance HCE and LHCE at room temperature are faced with high-viscosity challenges when applying them to low-temperature conditions. Molecular and electrolyte designs are therefore of necessity to be conducted.

A low-viscosity electrolyte is generally desired considering its benefits of high conductivity and good wettability.^[4,7] The intermolecular interactions largely determine the viscosity of liquid electrolytes. Therefore, only by tailoring the electrolyte compositions at the molecular level can an electrolyte recipe with appropriate viscosity be efficiently acquired. First, molecules containing fewer bulky functional groups are preferred. The interactions between solvent molecules are dominated by van der Waals forces which are mainly affected by molecular weight and polarity. Bulky functional groups induce strong van der Waals forces and high viscosity. For instance, DMC, EMC, and DEC share similar structures but the alkyl residues become larger from DMC to DEC, and so is the viscosity trend among them. Consequently, bulky groups such as ethyl groups, propyl groups, or longer chains are preferably precluded when selecting or designing solvent molecules. Second, a balance should be achieved between the viscosity and solvating ability of solvents. A polar solvent tends to possess a strong power to solvate ions because of the strong ion–dipole interaction.^[37] This favors a large charge carrier concentration and hence a high ionic conductivity. At the same time, the dipole–dipole interaction between solvents themselves becomes intense too, which raises the viscosity. The consideration of lowering the viscosity should be built on ensuring adequate solvating ability to comprehensively optimize electrolyte properties. Third, the solvating power of diluents should be promoted slightly. The ionic networks in LHCEs still produce a large viscosity and impede the motion of electrolyte species, especially ions. Plenty of room remains for delicate improvement in the solvating ability of diluents, lying between totally non-solvating chemicals and routine solvents. It is expected to preserve favorable solvation structures but break ionic networks further in this way. Then the viscosity can be reduced and ions can move freely.

Conclusion

An effective and reliable method, SOM, was developed to compute electrolyte viscosity by molecular dynamics simulations, and the relative errors of viscosities computed by this method with respect to experimental values are smaller than $\pm 5\%$ for most solvents. The molecular origin of viscosity was further systematically probed. The viscosities of both pure solvents and binary solvent mixtures exhibit an exponential relationship with the binding energy between solvent molecules, implying the internal correlation between the intermolecular interaction and viscosity. Besides, the viscosities of solvent mixtures do not follow the linear superposition of viscosities of individual solvents, which was also attributed to the variation of the intermolecular interactions. Salts increase electrolyte viscosity due to not

only the stronger cation–anion association than the solvent–solvent interaction but also the additional binding between cations and solvents. These interactions are gradually enhanced with increased salt concentrations. The low-viscosity diluents help alleviate the high viscosity of concentrated electrolytes by weakening the overall binding strength between electrolyte components, delivering reduced viscosities and accelerated ionic transport. The computational method proposed in this work affords an effective approach for acquiring the electrolyte viscosity and helps uncover the underlying correlation between intermolecular interactions and viscosity. The method coupled with the deep understanding of viscosity is promising in speeding up the rational design of molecules and electrolyte recipes for high-performance batteries.

Acknowledgements

This work was supported by the National Key Research and Development Program (2021YFB2500300), Beijing Municipal Natural Science Foundation (Z200011), National Natural Science Foundation of China (22109086, 22209093, 22209094, and 21825501), and Young Elite Scientists Sponsorship Program by CAST (2021QNRC001). The authors acknowledged the support from Tsinghua National Laboratory for Information Science and Technology for theoretical simulations.

Conflict of Interest

The authors declare no conflict of interest.

Data Availability Statement

The data that support the findings of this study are available on request from the corresponding author. The data are not publicly available due to privacy or ethical restrictions.

Keywords: Green–Kubo Relation • Lithium Battery Electrolyte • Molecular Dynamics Simulation • Screened Overlapping Method • Viscosity

- [1] X. Zeng, M. Li, D. Abd El-Hady, W. Alshitari, A. S. Al-Bogami, J. Lu, K. Amine, *Adv. Energy Mater.* **2019**, *9*, 1900161; M. Li, J. Lu, Z. Chen, K. Amine, *Adv. Mater.* **2018**, *30*, 1800561.
- [2] M. S. Ding, A. von Cresce, K. Xu, *J. Phys. Chem. C* **2017**, *121*, 2149–2153.
- [3] R. Tian, S.-H. Park, P. J. King, G. Cunningham, J. Coelho, V. Nicolosi, J. N. Coleman, *Nat. Commun.* **2019**, *10*, 1933.
- [4] M.-T. F. Rodrigues, G. Babu, H. Gullapalli, K. Kalaga, F. N. Sayed, K. Kato, J. Joyner, P. M. Ajayan, *Nat. Energy* **2017**, *2*, 17108.
- [5] Y. Liu, Y. Zhu, Y. Cui, *Nat. Energy* **2019**, *4*, 540–550.

- [6] A. J. Ringsby, K. D. Fong, J. Self, H. K. Bergstrom, B. D. McCloskey, K. A. Persson, *J. Electrochem. Soc.* **2021**, *168*, 080501.
- [7] H. Zheng, H. Xiang, F. Jiang, Y. Liu, Y. Sun, X. Liang, Y. Feng, Y. Yu, *Adv. Energy Mater.* **2020**, *10*, 2001440.
- [8] X. Cao, P. Y. Gao, X. D. Ren, L. F. Zou, M. H. Engelhard, B. E. Matthews, J. T. Hu, C. J. Niu, D. Y. Liu, B. W. Arey, C. M. Wang, J. Xiao, J. Liu, W. Xu, J.-G. Zhang, *Proc. Natl. Acad. Sci. USA* **2021**, *118*, e2020357118.
- [9] L. Chen, E. Bonaccorso, *Phys. Rev. E* **2014**, *90*, 022401.
- [10] T. R. Kartha, B. S. Mallik, *Mater. Today Commun.* **2020**, *25*, 101588; E. R. Logan, E. M. Tonita, K. L. Gering, L. Ma, M. K. G. Bauer, J. Li, L. Y. Beaulieu, J. R. Dahn, *J. Electrochem. Soc.* **2018**, *165*, A705–A716; P. Wang, A. Anderko, R. D. Young, *Fluid Phase Equilib.* **2004**, *226*, 71–82; S. Seki, K. Hayamizu, S. Tsuzuki, K. Takahashi, Y. Ishino, M. Kato, E. Nozaki, H. Watanabe, Y. Umebayashi, *J. Electrochem. Soc.* **2018**, *165*, A542–A546.
- [11] D. Nevins, F. J. Spera, *Mol. Simul.* **2007**, *33*, 1261–1266.
- [12] N. Yao, X. Chen, X. Shen, R. Zhang, Z.-H. Fu, X.-X. Ma, X.-Q. Zhang, B.-Q. Li, Q. Zhang, *Angew. Chem. Int. Ed.* **2021**, *60*, 21473–21478; N. Yao, X. Chen, Z.-H. Fu, Q. Zhang, *Chem. Rev.* **2022**, *122*, 10970–11021.
- [13] M. S. Green, *J. Chem. Phys.* **1951**, *19*, 1036–1046; R. Kubo, M. Yokota, S. Nakajima, *J. Phys. Soc. Jpn.* **1957**, *12*, 1203–1211; H. Mori, *Phys. Rev.* **1958**, *112*, 1829–1842.
- [14] M. Stengel, N. A. Spaldin, D. Vanderbilt, *Nat. Phys.* **2009**, *5*, 304–308.
- [15] M. P. Allen, D. J. Tildesley, *Computer Simulation of Liquids*, 2nd ed., Oxford University Press, Oxford, **2017**.
- [16] T. Chen, B. Smit, A. T. Bell, *J. Chem. Phys.* **2009**, *131*, 246101; J. F. Danel, L. Kazandjian, G. Zerah, *Phys. Rev. E* **2012**, *85*, 066701.
- [17] M. A. González, J. L. F. Abascal, *J. Chem. Phys.* **2010**, *132*, 096101; G.-J. Guo, Y.-G. Zhang, *Mol. Phys.* **2001**, *99*, 283–289.
- [18] G. S. Fanourgakis, J. S. Medina, R. Prosimi, *J. Phys. Chem. A* **2012**, *116*, 2564–2570.
- [19] T. Yamaguchi, H. Yamada, T. Fujiwara, K. Hori, *J. Mol. Liq.* **2020**, *312*, 113288.
- [20] C. Rey-Castro, L. F. Vega, *J. Phys. Chem. B* **2006**, *110*, 14426–14435.
- [21] Y. Zhang, A. Otani, E. J. Maginn, *J. Chem. Theory Comput.* **2015**, *11*, 3537–3546.
- [22] B. Hess, *J. Chem. Phys.* **2002**, *116*, 209–217.
- [23] D. J. Schroeder, A. A. Hubaud, J. T. Vaughey, *Mater. Res. Bull.* **2014**, *49*, 614–617.
- [24] L. Xia, B. Tang, L. Yao, K. Wang, A. Cheris, Y. Pan, S. Lee, Y. Xia, G. Z. Chen, Z. Liu, *ChemistrySelect* **2017**, *2*, 7353–7361.
- [25] E. M. Gosling, I. R. McDonald, K. Singer, *Mol. Phys.* **1973**, *26*, 1475–1484.
- [26] Y. Yamada, A. Yamada, *Chem. Lett.* **2017**, *46*, 1056–1064; J. Zheng, J. A. Lochala, A. Kwok, Z. D. Deng, J. Xiao, *Adv. Sci.* **2017**, *4*, 1700032; O. Borodin, J. Self, K. A. Persson, C. Wang, K. Xu, *Joule* **2020**, *4*, 69–100; Y. Yamada, J. Wang, S. Ko, E. Watanabe, A. Yamada, *Nat. Energy* **2019**, *4*, 269–280.
- [27] J. Qian, W. A. Henderson, W. Xu, P. Bhattacharya, M. Engelhard, O. Borodin, J. G. Zhang, *Nat. Commun.* **2015**, *6*, 6362.
- [28] J. Wang, Y. Yamada, K. Sodeyama, C. H. Chiang, Y. Tateyama, A. Yamada, *Nat. Commun.* **2016**, *7*, 12032.
- [29] N. Piao, X. Ji, H. Xu, X. Fan, L. Chen, S. Liu, M. N. Garaga, S. G. Greenbaum, L. Wang, C. Wang, X. He, *Adv. Energy Mater.* **2020**, *10*, 1903568.
- [30] S. Perez Beltran, X. Cao, J.-G. Zhang, P. B. Balbuena, *Chem. Mater.* **2020**, *32*, 5973–5984.
- [31] S. R. Chen, J. M. Zheng, D. H. Mei, K. S. Han, M. H. Engelhard, W. G. Zhao, W. Xu, J. Liu, J.-G. Zhang, *Adv. Mater.* **2018**, *30*, 1706102.
- [32] X. Chen, X.-Q. Zhang, H.-R. Li, Q. Zhang, *Batteries Supercaps* **2019**, *2*, 128–131; X. Chen, Q. Zhang, *Acc. Chem. Res.* **2020**, *53*, 1992–2002.
- [33] B. Wen, Z. Deng, P.-C. Tsai, Z. W. Lebens-Higgins, L. F. J. Piper, S. P. Ong, Y.-M. Chiang, *Nat. Energy* **2020**, *5*, 578–586.
- [34] X. Cao, H. Jia, W. Xu, J. G. Zhang, *J. Electrochem. Soc.* **2021**, *168*, 010522.
- [35] X. Ren, S. Chen, H. Lee, D. Mei, M. H. Engelhard, S. D. Burton, W. Zhao, J. Zheng, Q. Li, M. S. Ding, M. Schroeder, J. Alvarado, K. Xu, Y. S. Meng, J. Liu, J.-G. Zhang, W. Xu, *Chem* **2018**, *4*, 1877–1892.
- [36] R. B. Bird, W. E. Stewart, E. N. Lightfoot, *Transport Phenomena*, 2nd ed., Wiley, New York, **2002**.
- [37] R. Christian, W. Thomas, *Solvents and solvent effects in organic chemistry*, Wiley-VCH, Weinheim, **2011**.

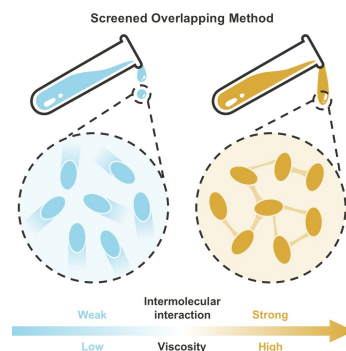
Manuscript received: April 15, 2023
Accepted manuscript online: May 12, 2023
Version of record online: ■■■, ■■■

Research Articles

Battery Electrolytes

N. Yao, L. Yu, Z.-H. Fu, X. Shen, T.-Z. Hou,
X. Liu, Y.-C. Gao, R. Zhang, C.-Z. Zhao,
X. Chen,* Q. Zhang* — e202305331

Probing the Origin of Viscosity of Liquid
Electrolytes for Lithium Batteries



A screened overlapping method (SOM) was developed to effectively compute the viscosity of liquid electrolytes. Based on this method, it is revealed that strong intermolecular interactions give rise to the high viscosity of liquid electrolytes and impede the motion of species in electrolytes.